Masses in periodic QED

Gideon Lana
School of Physics and Astronomy, Raymond and Beverly Sackler Faculty of Exact Sciences, Tel Aviv University, Tel Aviv 69978, Israel
(Received 14 March 1988)

Block renormalization-group techniques are used to study low-energy aspects of periodic QED in $2+1$ dimensions. We compute the masses of the symmetric and antisymmetric excitations. Our results exhibit the correct scaling behavior in the weak-coupling regime.

I. INTRODUCTION

Periodic QED (PQED) in two spatial dimensions on the lattice has acquired considerable attention, primarily because it is one of the simplest nontrivial gauge theories. In addition there is no phase transition between the weak-coupling and the strong-coupling regime. This feature qualifies this model as a testing laboratory for methods that aim at calculating the QCD spectrum which was the original motivation for introducing the lattice formulation for gauge theories.

The first ones who investigated the model were Polyakov,[1] who calculated the weak-coupling behavior by summing over topologies of a classical field, and Banks, Meyerson, and Kogut,[2] who used the Villain approximation of the Wilson action. They have shown that the string tension σ and the mass gap are finite for every nonvanishing value of the coupling constant, and vanish with an essential singularity in the $g \to 0$ limit.

Giving this model a rigorous treatment Göpfert and Mack[3] confirmed these results and found the string tension to obey the bound

$$\sigma a \geq C \frac{g^2}{\pi^2} M \ , \tag{1}$$

where M is their estimate for the mass gap,

$$M^2 a^2 = \frac{8\pi^2}{g^2} \exp\left[-2v(0) \frac{\pi^2}{g^2} \right] , \tag{2}$$

$v(0)$ is the inverse propagator in the limit of zero coordinate separation and C is a numerical constant.

Working with the Hamiltonian version, Suranyi[4] has obtained parallel results. Using a generalized WKB method he showed that the asymptotic weak-coupling behavior of the mass gap is

$$m^2 a^2 \sim \exp\left[\frac{-5.7 \pm 0.1}{g^2} \right] . \tag{3}$$

A slightly different estimate was obtained by a cluster expansion[5] and the more sophisticated dilute-gas approximation.[6]

Using a multiparameter variational wave function Heys and Stump[7] reproduced the expected scaling behavior by a Hamiltonian Monte Carlo calculation. Their trial wave function contains the ingredients needed to produce long-range correlations in the weak-coupling regime. Their fit to the mass gap over the range $\sqrt{3} \geq g^{-2} \geq 1.2$ gives

$$m^2 a^2 = \frac{500 \pm 30}{g^2} \exp\left[\frac{-4.97 \pm 0.05}{g^2} \right] . \tag{4}$$

This result is in excellent agreement with the one obtained by Hamer and Irving,[8] who used strong-coupling cluster expansion. This seems a bit surprising, since one expects that very large clusters (which correspond to high orders of calculation) are needed to see the correct subtle behavior of the mass in the weak-coupling limit. In particular, terminating such expansions after a few orders is equivalent, in some sense, to working on a lattice whose size just exceeds the largest computed cluster. In this state of affairs finite-size scaling effects may govern the results. Another serious defect of strong-coupling expansions is that very high orders are required to reproduce the harmonic-oscillator character of the weak-coupling limit.

II. THE METHOD

The standard lattice Hamiltonian for PQED in $2+1$ dimensions is

$$H = \frac{g^2}{2a} (H_E + x H_M) \ , \tag{5}$$

$$H_E = \sum_l E_l^2 = -\sum_l \frac{\partial^2}{\partial \theta_l^2} \ , \tag{6}$$

$$H_M = \sum_p (1 - \cos\theta_p) \ . \tag{7}$$

The Hilbert space is defined by the compact link variables θ_l. θ_p is the usual discrete version of the curl of the gauge field, and $x = 2/g^4$.

Clearly the link variables are not independent due to the Gauss law. However, in two dimensions the Gauss-law constraints can be eliminated from the problem by a transformation to the plaquette variables θ_p in terms of which Eq. (5) may be rewritten as

$$H = \sum_p H_p + \sum_{\langle pp' \rangle} V_{pp'} \ , \tag{8}$$

$$H_p = \frac{g^2}{2a} \left[-4 \frac{\partial^2}{\partial \theta_p^2} + x(1 - \cos\theta_p) \right] , \tag{9}$$

$$V_{pp'}=\frac{g^2}{a}\frac{\partial}{\partial\theta_p}\frac{\partial}{\partial\theta_{p'}}\ , \tag{10}$$

where the symbol $\langle pp'\rangle$ in (8) implies summation over all nearest-neighbor pairs of plaquettes.

Treating V as a perturbation, we will proceed as follows: For an arbitrary value of g diagonalize H_p, namely, solve the Mathieu equation

$$H_p\,|\,n_p\rangle=E_{n_p}^{(0)}\,|\,n_p\rangle\ . \tag{11}$$

Obviously the Hilbert space in the charge-free sector is spanned by the family of outer product states over the plaquette variables $|\{n_p\}\rangle\equiv\prod_p|\,n_p\rangle$.

In this infinite-spin Ising-type Hamiltonian the Block renormalization-group (BRG) method can be applied. This method was first presented by Drell, Weinstein, and Yankielowicz[9] for a simple $(1+1)$-dimensional Ising model. It has later been shown to be a very efficient tool for investigating a variety of statistical mechanics as well as field-theory models.[10]

Proceeding in the spirit of Ref. 9, one divides the lattice into four-plaquette blocks organized on a square. Grouping the Hamiltonian into a sum of an intrablock part and an interblock part that includes exactly half of the $V_{pp'}$ terms gives

$$H=\sum_{\text{blocks}}H_b+\sum_{\langle bb'\rangle}V_{bb'}\ , \tag{12}$$

$$H_b=\sum_{n_1n_2n_3n_4}(E_{n_1}^{(0)}+E_{n_2}^{(0)}+E_{n_3}^{(0)}+E_{n_4}^{(0)})\,|\,n_1n_2n_3n_4\rangle\langle n_1n_2n_3n_4\,|$$
$$+\frac{g^2}{a}\sum_{n_1n_2n_3n_4}\sum_{m_1m_2m_3m_4}[\delta_{n_1m_1}\delta_{n_2m_2}d(n_3,m_3)d(n_4,m_4)$$
$$+3\text{ similar terms}]\,|\,n_1n_2n_3n_4\rangle\langle m_1m_2m_3m_4\,|\ , \tag{13}$$

where

$$d(n,m)=\left\langle n\left|\frac{1}{i}\frac{\partial}{\partial\theta_p}\right|m\right\rangle\ . \tag{14}$$

At this stage one truncates the Hilbert space so that only a finite number of states substitutes for the infinite number we had for every block. This is equivalent to projecting our problem onto a generalized Ising model. Keeping two states at each plaquette gives, for example, a spin-$\frac{1}{2}$ form of Hamiltonian. It must be emphasized that for every value of the coupling constant one gets quite different parameters for the corresponding Ising model: i.e., different E's and different coupling d matrices. The simplest truncation procedure would keep a few lowest-energy states for every subblock.

By diagonalizing this matrix, we get a new basis of states, that we use to construct blocks of larger size. Here again for practical reasons one must truncate the Hilbert space. In addition, since we are interested only in the zero-momentum sector (i.e., only translation- and rotation-invariant states) we pick only the states which are singlets with respect to the transformations of the symmetry group of the square D_4. An alternative and much more efficient way is to limit ourselves to the zero-momentum sector by working from the beginning in a D_4 symmetrized basis of states at each step. The elimination of states which are not D_4 singlets does not alter the results, since at each step the block Hamiltonian is a singlet operator and therefore there are no nonzero matrix elements connecting different D_4 representations.

Very few iterations are needed until the vacuum energy density $\mathcal{E}$ stabilizes. The masses need more iterations before stabilizing, especially for lower values of g^2. At this stage, after performing n iterations we take $\mathcal{E}=E_0^{(n)}/4^n$, $M_a=E_1^{(n)}-E_0^{(n)}$, and $M_s=E_2^{(n)}-E_0^{(n)}$ as representing the vacuum energy density of the infinite lattice and the masses of the antisymmetric and symmetric excitations. The definite charge-conjugation symmetry of the states is guaranteed since this symmetry is respected at every step of our procedure.

III. THE RESULTS

The quantity which is the easiest to compute is the vacuum energy. Although in itself it is of very little physical interest, it can serve as a general test for the method by comparing it to the exact values both at $g^2\to\infty$ and at $g^2\to0$. One can keep only the lowest three states at each subblock (making a $3^4\times3^4$ matrix of product states or a 21×21 matrix in the symmetrized basis), to get fair results. These are shown in Fig. 1 for four consecutive iterations.

Figure 2 shows the final result for working with six states per subblock (making a 231×231 matrix in the symmetrized basis), together with the specific heat $C=-\partial^2\mathcal{E}/\partial y^2$ where $y=2/g^2$. Though vanishingly small near the origin, the specific heat is non-negative for all of the g^2 range. A linear fit to the vacuum energy density gives

$$\mathcal{E}=0.965-0.122g^2+O(g^4) \tag{15}$$

which is in fair agreement with the weak-coupling perturbation expansion:

$$\mathcal{E}=0.958-0.114g^2+O(g^4)\ . \tag{16}$$

However, when computing the mass gap there is a considerable improvement of the results as more states are

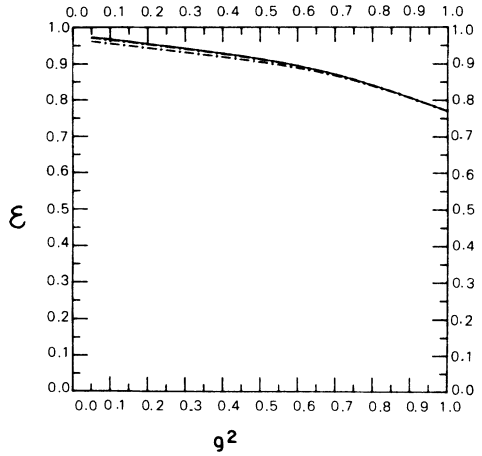

FIG. 1. Four consecutive iterations of the vacuum energy density $\mathcal{E}$ plotted against the coupling constant. One clearly sees the rapid convergence of this quantity.

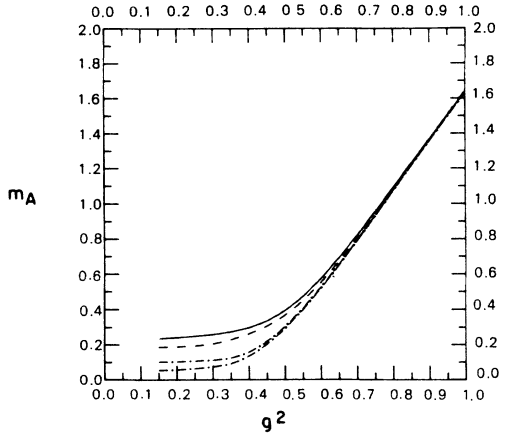

FIG. 3. The final results for the mass gap M_a for retaining three, four, five, and six states per subblock. Clearly, as we work in a larger truncated Hilbet space, the system freezes at lower values of the coupling constant.

being kept. The volume of the truncated Hilbert space becomes a crucial issue when working in the weak-coupling regime.

Figure 3 shows the final results for three, four, five, and six states kept at each subblock every iteration. The improvement when going to seven states per subblock (meaning that 406×406 matrices are to be diagonalized) is negligible although the required computer time increased by an order of magnitude.

The excellent agreement of the different curves of Fig. 3 down to quite low values of g^2 suggests they can be trusted over a wide range of values of the coupling constant. However, in all these cases one notices that the mass remains constant for small g^2 values. This is an artifact that becomes less pronounced as a larger subspace of the complete space of interactions is used in the BRG process. This phenomenon presumably originates from the freezing of the degrees of freedom, i.e., replacing an infinite number of states over each block (corresponding to the continuous symmetry) by a finite number of them (corresponding to a discrete group). A similar effect is observed when trying to perform a Monte Carlo calculation of a continuous group theory using one of its discrete subgroups.

Using a more physical truncation criterion improved the situation considerably. Instead of using a brute cutoff of subblock states, we retained a fixed number of block symmetrized states—the ones with the lowest unperturbed block energies.

Figure 4 shows our final results for M_a and M_s. One can gain some insight about the charge-conjugation symmetry of the states by looking at the one-plaquette prob-

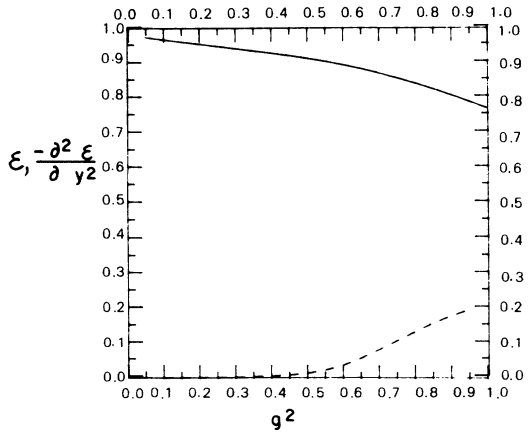

FIG. 2. The final result for the vacuum energy density $\mathcal{E}$ (solid line) and the specific heat (dashed line) obtained by diagonalizing a 305×305 matrix every iteration. After the seventh iteration, $\mathcal{E}$ became invariant to the blocking procedure.

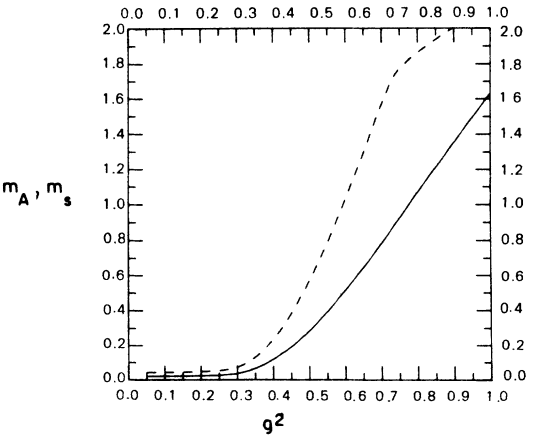

FIG. 4. Our final results for M_a (solid line) and M_s (dashed line). These results were obtained by working each iteration in a Hilbert space of 405 symmetrized block states having the lowest unperturbed block energies.

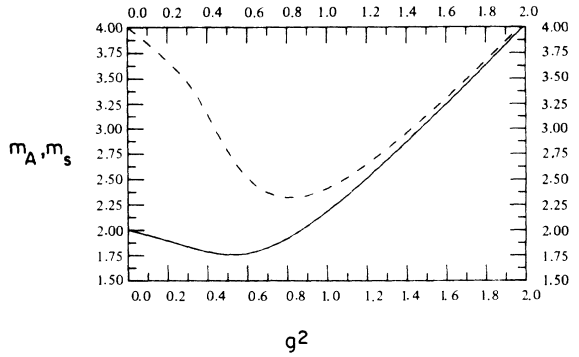

FIG. 5. The masses of the symmetric and antisymmetric states of the one-plaquette problem in units of $1/a$.

lem (which is sometimes called the lattice oscillator). The spectrum of this simple model (Fig. 5) resembles strikingly that of the infinite lattice down to quite low values of the coupling constant. At the strong-coupling limit the symmetric and the antisymmetric excitations are degenerate. For any finite g^2 the antisymmetric excitation lies lower than the symmetric excitation. At $g^2=0$ the one-plaquette problem turns into a harmonic-oscillator problem, so that the ratio of the vacuum, the antisymmetric and symmetric energies is 1:3:5, and the ratio of the masses is identically 2.

In Fig. 6 we plotted the scaling ratio M_s/M_a. It should be of no surprise that we do well in the crossover regime and that in the $g\to\infty$ limit we have $M_s/M_a\to 1$. More impressive is the fact that we actually get the expected ratio $M_s/M_a=2$ in the weak-coupling limit. We thus verify the conclusion of Göpfert and Mack,[3] that the continuum limit of the model is a theory of free, massive bosons. Thus for low-g^2 values the symmetric excitation corresponds to two weakly bound antisymmetric states. Furthermore, the point where the symmetric state ceases to be stable is clearly seen to be located at

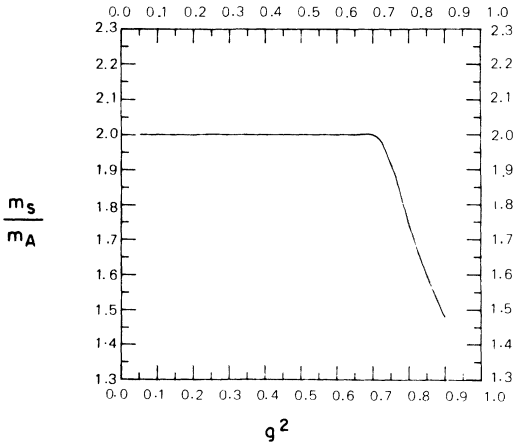

FIG. 6. The scaled ratio M_s/M_a. Our exact $g\to 0$ result is within 0.5% to the theoretical value at this limit. Notice the transition point at $g^2=0.71$, where the symmetric state ceases to be stable.

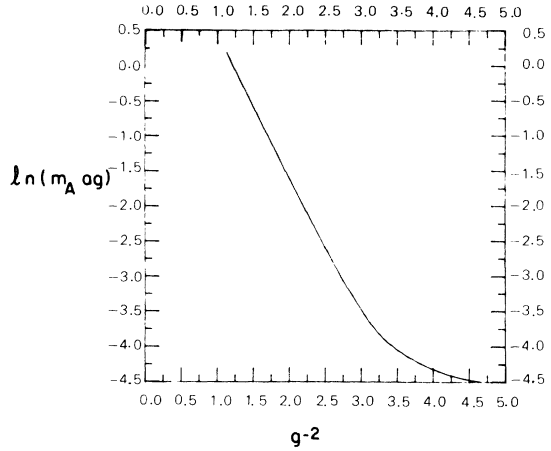

FIG. 7. This plot of $\ln(M_a ag)$ vs g^{-2} verifies in a most explicit manner the scaling nature of the mass gap. The solid line is the result of the two-step iteration procedure. A linear fit to this curve led to the estimate of Eq. (17).

$g^2=0.71$.

The disappearance of the bound state does not yet ensure that our results actually reflect the weak-coupling features of the theory. Figure 7 shows the scaling nature of the mass gap itself. The points align on a straight line down to very low values of g^2. A straight-line fit to the points with $3>g^{-2}>1.2$ gives

$$m^2a^2=\frac{145\pm 15}{g^2}\exp\left[-\frac{4.1\pm 0.2}{g^2}\right]. \tag{17}$$

As a final test of the validity of our results, we performed a similar calculation, in which every iteration was divided into two steps: In the first step one groups two square subblocks and diagonalizes the corresponding block Hamiltonian; in the second step we regain the x-y symmetry by performing a similar blocking in the perpendicular direction. Clearly the symmetry group $Z_2\times Z_2$ we now have per iteration is a subgroup of D_4 we had in the original procedure. However, here the renormalization-group parameters "flow" in smaller steps. Practically it means we can work in a much larger space of interactions which makes the whole process more exact. The results of the two blocking procedures are almost identical down to $g^2\simeq 0.3$. But as expected, in the two-step-iteration algorithm, the system "freezes" at much lower values of the coupling constant. The overall behavior of the mass gap [Eq. (17)] remains, however, unchanged.

IV. SUMMARY AND CONCLUSIONS

We have carried out a calculation of the energies of the lowest-lying excitations in PQED in $2+1$ dimensions. This nonperturbative method uses no artificial apparatus in order to extrapolate to the weak-coupling regime (e.g., Padé approximants). Rather our results are computed separately for every value of the coupling constant. Here we see that M_a and M_s start scaling at the crossover re-

gime in contradistinction with an earlier conclusion.[11]

Our starting point is a set of wave functions which describe the exact local correlationless excitations. By iterating the blocking procedure, correlations of arbitrary size are produced. Large loops of electric flux that are being successively built in the wave function reproduce well the disorder in the weak-coupling region: This feature and the astronomic number of parameters that are being naturally determined by the procedure, are believed to be the key to its success.

The uniqueness of our results is that they actually verify the scaling nature of the masses, i.e., we actually see that the two lowest masses M_a and M_s exhibit the same exponential behavior, giving the correct scaling ratio $M_s/M_a=2$. Moreover, our results for the scaling nature of the mass gap penetrate much deeper into the weak-coupling regime than earlier computations.

We are not too puzzled finding that the prefactor of the mass behavior obtained by our calculation does not match the variational prefactor.[5] It is known to be rather sensitive to the approximation used.

Because of its Abelian nature and the fact that it naturally decomposes into the plaquette variable, the method is particularly well suited for $(2+1)$-dimensional PQED. Using a similar technique to other more physically interesting theories (for example, QCD) is clearly nontrivial. Even its generalization to PQED in three spatial dimensions is in itself quite a challenge.

ACKNOWLEDGMENTS

Thanks are due to Y. Shadmy for help in the preliminary computational work and to D. Horn for his guidance. This work was supported in part by the Israel Academy of Science.

[1]A. M. Polyakov, Phys. Lett. **59B**, 82 (1975); Nucl. Phys. **B120**, 429 (1977).

[2]T. Banks, R. Meyerson, and J. Kogut, Nucl. Phys. **B129**, 493 (1977).

[3]M. Göpfert and G. Mack, Commun. Math. Phys. **82**, 545 (1982).

[4]P. Suranyi, Nucl. Phys. **B225** [FS9], 538 (1983).

[5]P. Suranyi, Phys. Lett. **122B**, 279 (1983).

[6]H. G. Evertz and D. Horn, Phys. Rev. D **30**, 2664 (1984).

[7]D. W. Heys and D. R. Stump, Nucl. Phys. **B285** [FS19], 13 (1987).

[8]C. J. Hamer and A. C. Irving, Z. Phys. C **27**, 145 (1985).

[9]S. Drell, M. Weinstein, and S. Yankielowicz, Phys. Rev. D **16**, 1769 (1977).

[10]S. Drell, B. Svetitsky, and M. Weinstein, Phys. Rev. D **17**, 523 (1978); R. Jullien and P. Pfeuty, Phys. Rev. B **19**, 4646 (1979); J. Hirsch, *ibid.* **22**, 5259 (1980); G. Spronken, R. Jullien, and M. Avignon, *ibid.* **24**, 5356 (1981); E. Fradkin and S. Raby, Phys. Rev. D **20**, 2566 (1979).

[11]D. Horn, G. Lana, and D. Schreiber, Phys. Rev. D **36**, 3218 (1987).